Performance Analysis of Heterogeneous Networks in the presence of Deliberate Jammers using Reverse Frequency Allocation

By

Muhammad Ihsan Ur Rehman

00000320878

Supervisor

Dr. Abdul wakeel

Department of Electrical Engineering

Military College of Signals (MCS)
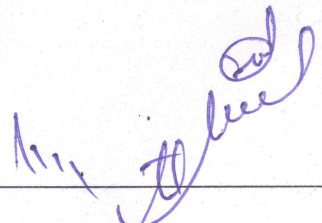
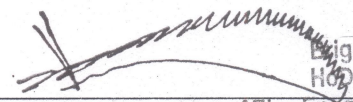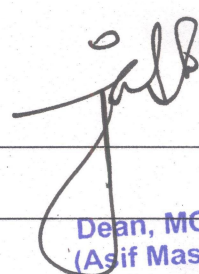National University of Sciences and Technology (NUST)

Islamabad, Pakistan

September 2023

THESIS ACCEPTANCE CERTIFICATE

Certified that final copy of MS/MPhil thesis written by Miss **NS Muhammad Ihsan Ur Rehman** Registration No. **00000320878** of **Military College of Signals** has been vetted by undersigned, found complete in all respect as per NUST Statutes/Regulations, is free of plagiarism, errors and mistakes and is accepted as partial, fulfillment for award of MS/MPhil degree. It is further certified that necessary amendments as pointed out by GEC members of the student have been also incorporated in the said thesis.

Signature: _____

Name of Supervisor **Asst Prof Abdul Wakeel, PhD**

Date: _____

Signature (HoD): _____

Date: _____

Signature (Dean): _____

Date: ____14/9/23____

Brig
Dean, MCS (NUST)
(Asif Masood, Phd)

Dedication

- I dedicate this thesis to the two pillars of my life, my loving family and my dearest friends. To my family, whose unwavering support, encouragement, and sacrifices have been my constant motivation, I offer my deepest gratitude. Your belief in my abilities has propelled me to reach this milestone. To my friends, for the laughter, camaraderie, and understanding during both the challenging and joyous moments of this journey, I am immensely thankful. This work is a reflection of the love, resilience, and friendships that have sustained me throughout this academic pursuit.

Declaration

I, *Muhammad Ihsan Ur Rehman* declare that this thesis titled "Performance Analysis of Heterogeneous Networks in presence of Deliberate Jammers using Reverse Frequency Allocation" and the work presented in it are my own and has been generated by me as a result of my own original research.

I confirm that:

1. This work was done wholly or mainly while in candidature for a Master of Science degree at NUST

2. Where any part of this thesis has previously been submitted for a degree or any other qualification at NUST or any other institution, this has been clearly stated

3. Where I have consulted the published work of others, this is always clearly attributed

4. Where I have quoted from the work of others, the source is always given. With the exception of such quotations, this thesis is entirely my own work

5. I have acknowledged all main sources of help

6. Where the thesis is based on work done by myself jointly with others, I have made clear exactly what was done by others and what I have contributed myself

Muhammad Ihsan Ur Rehman,

00000320878

Acknowledgement

- In completing this thesis, I am deeply grateful to the numerous individuals and organizations who have supported me on this academic journey. First and foremost, I extend my sincere appreciation to my thesis advisor, Dr. Abdul Wakeel, for unwavering guidance, patience, and expertise. I would also like to thank my thesis committee, Dr. Mir Yasir Umair, Dr. Mehmood Alam and Major Muhammad Qasim for their valuable insights and feedback. My heartfelt thanks go to my family for their enduring encouragement and belief in me. I am also indebted to my friends, colleagues, and research participants who contributed to this study. Lastly, I want to express my gratitude to Military College of Signals [NUST] for providing access to its libraries, research facilities, and academic resources, which were instrumental in conducting this research. This thesis is a culmination of the collective support and encouragement of these exceptional individuals and institutions.

- Above all thanks to Allah Almighty for everything.

Abstract

Future wireless communication networks are envisioned as multi-tier Hetnets, where small base stations (sBSs) are strategically deployed within the macro base station's (mBS) coverage area. This deployment strategy aims to optimize spectrum utilization and, consequently, minimize coverage gaps. Nevertheless, the performance of Hetnets is notably compromised by the presence of inter-cell interference (ICI). Moreover, the performance is further degraded when a deliberate jammer is used by an attacker having adequate information about the network parameters. The extent to which the performance can be degraded highly depends on the proximity of the jammer from the target as well as its transmit power. In HetNets, mBS has higher transmit power as compared to the sBS. Therefore, many users connect to the mBS resulting in an unbalanced load distribution.In order to achieve load balancing, users originally connected to the mBS are redirected to the sBS. However, this transition introduces interference in the communication due to the high transmit power of the mBS. Hence, we need interference management techniques that countermeasure the interference effect in the network as well as user association techniques for efficiently available resource utilization. This study proposes reverse frequency allocation (RFA) for Hetnets with deliberate jammers. RFA has been found to be an efficient solution for alleviating the effect of ICI and deliberate jammer interference (DJs-I). The available band in RFA is divided into sub-bands which are dis-jointly used by the mBS and the sBS in disjoint regions. RFA, therefore, efficiently reduces interference in the HetNets as well as accomplishing loading balancing. The proposed system model deploying RFA in the presence of DJs has been evaluated both analytically and with the assistance of simulation. Simulation outcomes show that our proposed solution has improved uplink (UL) coverage performance due to high interference mitigation (i.e., DJs-I and ICI) and load balancing as compared to the systems without RFA.

Contents

CONTENTS

List of Figures

List of Abbreviations

HetNet   heterogeneous cellular network

DJs   deliberate jammers

DJs-I   deliberate jammers interference

ICI   inter cell interference

SFR   soft Frequency Reuse

sBS   small base station

UL   Up-link

mBSs   macro base stations

RFA   reverse frequency allocation

U-HetNet   uniform heterogeneous cellular network

OFDMA   Orthogonal frequency division multiple access

NU-HetNet   Non Uniform Heterogeneous Cellular Network

DL   Downlink

M-EUs   MBS edge-users

FFR   Fractional Frequency Reuse

SIR   Signal-to-interference ratio

LT   Laplace transform

IHPPP   Independent Homogeneous Poisson Point Process

WiMAX   Worldwide Interoperability for Microwave Access

CHAPTER 1

Introduction

Recently, there has been an exponential increase in data rate requirements due to the invention of online games, conference calls, and video streaming. To cope with public demands, the future wireless communication systems are aimed to increase the system capacity many folds as compared to the 4G communications systems [1]. To boost the system capacity and spectral efficiency, 5G communication networks are evolving from Homogeneous networks to Heterogeneous Networks (HetNets) by integrating different communication technologies, such as IoT, vehicular Networks, Device-to-Device (D2D) communications, Machine-to-Machine (M2M) communications, e.t.c., under one paradigm.HetNets are therefore considered to be the futuristic networks that will offer broader services to the users.

1.1 Concept of HetNets

Hetnet is a paradigm considered for future wireless communication technologies to cater to high data rates, flexibly. The HetNets integrate different wireless networks having different constraints to form one access network. An extensive survey on Hetnets, its deployment, advantages, and capacity analysis can be found in [1]. Consider a two-tier HetNet where within the mBS coverage area ultra-dense sBSs are deployed, as shown in Fig. 1.1. Such a structure, thus, significantly improves the network coverage and bandwidth utilization. Some well-known benefits of
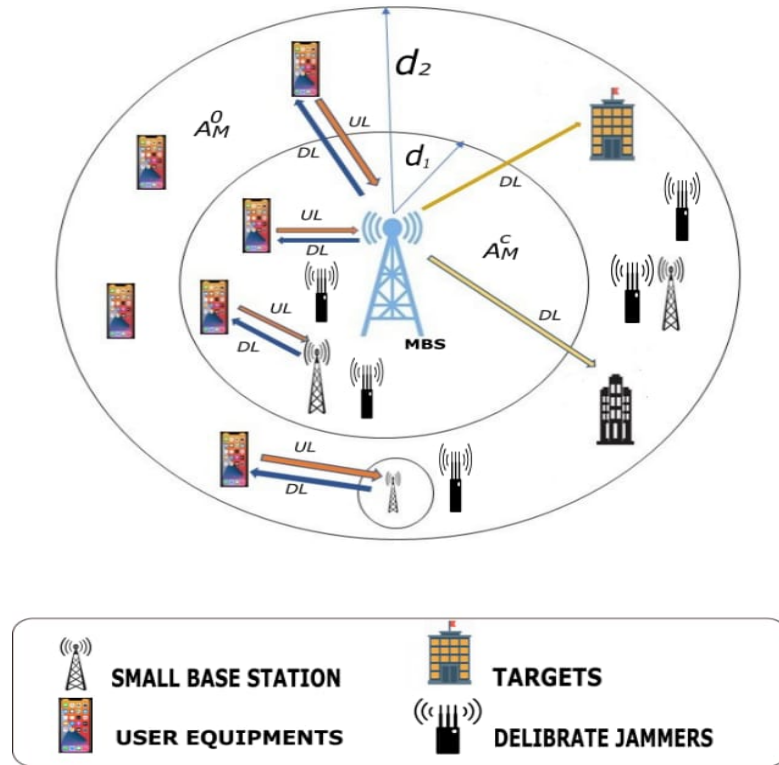
Figure 1.1: The proposed two-tier HetNet system model featuring Radio Frequency Allocation (RFA) and Deliberate jamming.

HetNets are:

- **Increasing system capacity:** By harnessing the capacity of each individual wireless access network within the designated coverage area, the entire system can accommodate a substantial user population. Offering alternative access points (APs) during periods of network overload, therefore, the likelihood of new / hand-off calls being blocked or dropped is significantly reduced.

- **Increasing system coverage:** Combining cellular mobile networks with WiFi, for example, can cover a broader geographical area.

- **User satisfaction:** A specific goal from the users can be accomplished by exploiting the differences in various technologies as well as data rates. Wireless Local Area Networks (WLANs) or picocells, for example, are frequently used to provide access in hotspot areas such as shopping malls, stadiums,

and restaurants, whereas cellular mobile networks are employed to provide user mobility.

- **Ultra-dense network:** Deploying closely spaced small cells will help in accommodating a large number of users having various power levels to access the network.

- **Offering end-users varying access costs:** Different end-users with specific demands can pay differently by attaining different data rates through wireless access depending on their status, economic circumstances, employment, as well as their necessities.

Hetnets integrate different access networks, therefore, there is a dire need to have a well-established user association and scheduling system. For example, in a two-tier HetNet sBSs are deployed densely in mBS covering region. As mBS transmits at higher power, users from the sBSs get connected to the mBS, resulting in an unbalanced load in the network which causes interference in communications. Therefore, we need user association and scheduling schemes that can keep the network balanced.

1.2 OFDMA

For simultaneous transmission HetNets use orthogonal frequency division multiple access (OFDMA) techniques, where different users are assigned a set of sub-carriers which are orthogonal to each others which thus helps in mitigating the intra-cell interference (ICI). However, ICI still remains a major performance limiting factor for HetNets, especially for mBS edge users (M-EUs) it greatly reduces the UL coverage. [2, 3].

1.3 Denial-of-service (DoS) attack

As communication is becoming increasingly important in our daily lives, we are getting more vulnerable to DDoS attacks that might disrupt our communications. To accomplish this goal, the attacker must acquire information about the network's characteristics, including transmission power, duration, and user locations. Armed with this data, the attacker can interfere with the legitimate communications within the network. The sheer number and variety of attack and defense strategies are astounding [4]. Low user transmit power levels make UL communications more vulnerable to DDoS assaults [5], [6]. As a result, this research looks into DJ attacks to see if they can lower a target's UL SIR [7].

1.4 Deliberate jammers

Hetnets integrate different wireless technologies under one paradigm. Therefore, they are prone to deliberate jammers for DDoS attacks, which, transmit high power noise signal in the same band as used by the legitimate user transmitting at low power in the UL coverage. The multitude of the deliberate jammers interference (DJs-I) significantly depends on two factors, their transmit powers and their proximity to the target. For DJs to be effective, they are deployed in large number transmitting at higher powers and placed in the vicinity of the targeted user.Additionally, in this research, it is assumed that the DJs possess essential network parameters like the target's location, transmit signal power, and the frequency band being utilized [8–10].

1.5 Inter cell interference

Because of their tractability and ease of analysis, IHPPPs is commonly used to distribute sBSs, mBSs, and individuals in HetNets [11–13]. The use of orthogonal frequency division multiplexing yields limited ICI in HetNets, however, it is still

the primary factor which degrades the performance [2, 14]. Users and mBSs are deployed by IHPPP in NU-HetNets, whereas sBSs are distributed via the Poisson hole process. NU-HetNets result in a lower ICI, which increases network coverage performance [3, 15].

1.6 Interference Reduction Techniques

Different interference mitigation schemes have been proposed by different researchers, the well known amongst them are soft frequency reuse (SFR) [16], fractional frequency reuse (FFR) [17], and reverse frequency allocation (RFA) [2, 17]. SFR system is based on frequency reuse, it, therefore, yields higher spectral efficiency. Within the framework of FFR, the available bandwidth is partitioned into sub-bands, resulting in reduced interference as a consequence [18]. RFA is a well known dynamic resource management system which mitigates the interference [2]. Radio Frequency Allocation (RFA) enhances the efficient utilization of maximum bandwidth within a cell, benefiting both the mBS and sBS. As a result, RFA provides superior spectral efficiency compared to FFR and SFR.

1.7 Suggested Work

In this research, we propose deployment of RFA in HetNets to mitigate the effect of ICI as well as DJs-I, thereby, improving the UL coverage performance. Moreover, we delve into the assessment of uplink (UL) coverage in Hetnets while considering deliberate jamming interference and Inter-Cell Interference (ICI). The positions of users as well as base stations is carried out using independent homogeneous Poisson point process (IHPPP) [13, 19–21].

1.8 Contributions and Objectives

The research objectives of the suggested work are following :

1. Investigation of the effects due to interference generated by the deliberate jammers in HetNets.

2. Calculation of the mathematical/ analytical expression for the UL coverage probabilities with RFA.

3. Investigation of Uplink coverage in the presence of deliberate jammers and ICI.

4. Analysis of UL coverage of the proposed model deploying RFA versus different network parameters, i.e., sBSs density, DJs-I, and SINR.

5. Deployment of RFA scheme in Hetnets for load balancing and interference mitigation due DJs and ICI.

1.9 Thesis Organization

Chapter 1 serves as an introduction to the problem and provides an overview of the thesis. Chapter 2 offers a comprehensive literature review encompassing various stages and aspects of the thesis, including an exploration of the research problem and key concepts. Chapter 3 discusses the system model used in this thesis. In chapter 4, coverage probability for UL has been calculated. Chapter 5 showcases the presentation and comparative analysis of detailed experimental results, accompanied by discussions. Chapter 6 then concludes the project and outlines future prospects.

CHAPTER 2

Literature Review

2.1 Jamming

Wireless networking plays a pivotal role in realizing ubiquitous computing, where network devices integrated into the environment ensure continuous connectivity and services, ultimately enhancing the quality of human life. However, contemporary wireless networks are susceptible to jamming technology, primarily because of the exposed nature of their wireless links. In [21], the authors have conducted comprehensive research on various jamming techniques, including equalization jammers, automatic gain control jammers, wideband jammers, and partial band jammers. The authors concluded that, for jamming advanced communication networks, the attackers need sophisticated jammers. The outcome demonstrates that, with severe performance degradation of MIMO systems, the DJs need to transmit at very high power. In [22], for better analysis of the coverage probability, the authors have split the coverage area of the mBS into two distinct zones: an outer cell area and an inner cell area. Their investigation unveiled that as users move into the inner cell area, they encounter substantial interference due to their proximity to the mBS, whereas those positioned in the outer cell area contend with a diminished Signal-to-Interference-plus-Noise Ratio (SINR) owing to their greater distance from the source. This is because the mBS exhibits a robust signal transmission within the inner cell area, resulting in reduced coverage for the sBSs

positioned within this inner cell area.

In [23], the authors have analyzed Multiple Input and Multiple Output (MIMO) networks under the influence of advanced jamming attacks. The findings suggest that there is a deterioration in network performance due to an escalation in jammer transmissions.A detailed comparison of different jamming schemes utilized in MIMO networks has also been carried out. The jammers can significantly degrade network performance by increasing their transmit power levels, according to their proposed model. Moreover, for different MIMO scenarios, the effectiveness of various jamming attacks is also analyzed.

In [24], the authors have designed an advanced receiver that effectively mitigates the effects of jamming on UL system of massive MIMO networks. The authors have assumed the degrading property of jammers in both pilot and data transmission phases. Their proposed scheme estimates the jamming channel along with the legitimate channel in the pilot phase, which is then used for building filters that neutralize jamming effects on the receiver.

2.2   Anti Jamming

In [25], a survey of several jamming and anti-jamming strategies was conducted. The authors examine various types of jammers as well as placement strategies to make the jammers more effective. On the target, different jamming attacks have varied impacts. For example, continual jammers use all available resources to jam the network without causing any interruptions. A reactive jammer, on the other hand, is better suited to a network with limited resources since it attacks the target only when a specified condition is met. A low-power jammer is difficult to detect; conversely, a high-power jammer will easily be spotted but will be able to jam the majority of the network. The location of the jammer is also essential in boosting the jamming effects. Anti-jamming measures can lessen the impact of the jammers greatly. Moving from a jammed channel to a non-jammed channel or from a jammed area to a non-jammed area are two strategies used to mitigate the

effects of jammers. It is simple to detect the existence of jammers, however, it is more difficult to determine the type of jammer. When compared to static nodes, anti-jamming for mobile nodes is more complex.

In [26], to layer 2 the authors added an HARQ whereas, layer 1 was equipped with an anti-jamming SIMO. In uplink video communication networks, the authors present an anti-jamming subcarrier/power allocation technique for hybrid automatic repeat request-based SIMO OFDMA. The proposed technique enhanced the peak signal-to-noise ratio by almost 11 dB. By the inclusion of HARQ , the peak signal-to-noise ratio was increased by roughly 2 dB.

2.3   Use of Reverse Frequency Allocation

By splitting the cell into distinct spatial regions and distributing frequencies appropriately, the RFA system assures inter-cell orthogonality. RFA encourages spectrum sharing, increases data transmission speed, and reduces MBS interference. The reverse frequency allocation approach (RFA) was employed to mitigate a significant source of interference. It involved partitioning the macro cell into non-overlapping segments and implementing complementary spectrum allocation between macrocells and femtocells. By harnessing RFA and its variations, along with established stochastic geometry techniques, we derived explicit formulas for both coverage probability and rate coverage in a two-tier cellular network. Two non-overlapping zones have been created using the mBS coverage region for RFA employment in HetNets, consisting of an inner region, A_k^c, and an outer region, A_k^o, $\forall k \in \{\text{M, S}\}$ [14, 27].

To mitigate ICI and load balancing, RFA was used by the authors in [14]. The authors showed that implementing their proposed setup improves coverage performance for mBS edge users significantly. Variants of RFA are presented in [28], as a way to improve network coverage. The authors have developed a hybrid RFA system that amalgamates the advantages of various other schemes. Through their data, the authors demonstrate how good resource usage causes the RFA variations

to significantly enhance coverage.

2.4   HetNets Model

The coverage region of mBS comprises many sBSs in order to boost capacity and network coverage in HetNets. The addition of additional sBSs, on the other hand, increases interference and complexity, making analysis and simulation more difficult. The author divides HetNets into closed and open access networks in [29]. Users' access to restricted access networks is limited to a single tier/BS, whereas users in open access networks have access to all BS across the whole network. Massive MIMO has also been considered in HetNets and homogenous systems by the authors.

MIMO with fixed cell size HetNets were modeled in [30] as well as single and multi-tier network comparisons. However, for user interaction with the BS, fixed distances were expected, which is not practicable. The use of zero-force precoding in multi-antenna HetNets has been explored in [31]. Using rate per user and coverage probability, a comparison of open and closed access was made. Various multiple antenna methodologies were used to calculate the system's performance. Interference mitigation in HetNets' uplink channel has been addressed in [32] by managing power and allocating specific resources to each user. The implementation of a semi-orthogonal allocation scheme resulted in less interference, and efficient power allocation resulted in an increase in system capacity.

In [33], authors have formed a HetNet by using one mBS and multiple sBSs having antennas of large scale employing hybrid digital and analog beam forming. Near-optimal results were obtained by use of only four RF chains. Moreover, the computational complexity was also significantly reduced.

The authors of [34], created a HetNet using one MBS and numerous SBSs with large-scale antennas and hybrid digital and analogue beam shaping. Only four RF chains were used to achieve near-optimal performance. Furthermore, the computational complexity was lowered greatly.

Femtocells are deployed inside the broadcasting area of mBSs. Femtocells have a coverage range of 10 to 100 meters and are known as eNBs for LTE when deployed indoors. Femtocells are cost-effective, low-power, low-complexity, small-scale base stations. One of the most appealing features of femtocells is that they can be seamlessly integrated with current cellular networks to provide reliable indoor coverage.

They are the size of a home router, and their deployment has increased dramatically in recent years due to the ease with which subscribers can install them[35]. As the femto cells are in small size and small cell networks use less power, they have a long battery life and can be proven to be an energy efficient option. Femtocells offer coverage to users within their designated areas, thereby relieving the burden on macro cell base stations in high-traffic zones. Due to the short proximity between the small cell and the subscriber, there is minimal power loss and reduced interference.

In [36], a two-tier HetNet model with intra-tier interdependence was introduced, featuring the deployment of Macro Base Stations (MBSs) through a Poisson point process, and Femto Base Stations (FBSs) organized using a Matern cluster process. The study derived precise equations for interference and outage probability, considering the distance between a user's device and the serving Base Station (BS). The results revealed that small cells boost per-user capacity and area spectral efficiency, yet they do not alleviate the problem of network outages.

2.5 Small Cell Networks

Increased interference occurs when numerous BSs are introduced into Hetnets.Consider aspects such as interference, cell size, UL power management, and deployment strategy for optimising the performance of a network with small cells [37]. The power of user equipment is a substantial contributor to interference in small cells. Authors in [37]found that in uniformly dispersed tiny cells, 18 dBm power of user equipment generated better outcomes than 23 dBm.

2.6 Multi-Slope Path Loss Model

One approach to harnessing the advantages of HetNets is to divert traffic towards small cells [38]. A commonly employed approach for user association involves using a single-slope path loss model. Due to the increasing network density and the presence of asymmetrical cell patterns, the precision of the single-slope path loss model is diminishing. In this research, the authors explored a model for deploying femtocells alongside macro cells in downlink HetNets and advocated the adoption of a dual slope path loss model. The findings demonstrated that employing a dual slope path loss model enhances system performance by enabling a greater offload of traffic from macros to femtocells.

Using a single path loss model can lead to discrepancies in received and interference powers when compared to actual values. The authors of [39], discussed a multi-slope route loss model with changing path loss exponents for different distance ranges. The expressions for Signal to Interference Ratio (SIR), Signal to Noise Ratio (SNR), and Signal to Interference Noise Ratio (SINR) have been derived. Based on the calculations, as network density increases, the SIR decreases, while the SNR increases. Moreover, at a particular finite density, the SINR attains its maximum value.

2.7 Interference management

To improve interference management, a soft frequency reuse approach can be applied [40]. In [40], the authors show numerically that soft frequency reuse outperforms frequency resource partitioning in every load state. Soft frequency reuse can also help to increase the average user rate.
Because of its bandwidth efficiency and OFDMA appropriateness for cellular networks, the fractional frequency reuse approach helps reduce interference [41]. In [41], the authors also conducted a comparison between the strategies of fractional frequency reuse and soft frequency reuse. The findings indicate that fractional fre-

quency reuse outperforms soft frequency reuse in terms of Signal-to-Interference Noise Ratio (SINR) and rate coverage probability, while soft frequency reuse surpasses fractional frequency reuse in terms of spectral efficiency.

2.8 NU-HetNets

NU-HetNets deploying SFR were studied by the authors in [23]. The authors have developed coverage probability equations for both U-HetNets and NU-HetNets. The simulation results provided in [23] show a significant improvement in the broadcasting area due to the implicit reduction in ICI.

In [42], a unique SBS deployment technique is presented, in which the SBSs are fueled by sustainable energy sources. The writers dubbed this method "off-grid NU-HetNets," as the grids were not plugged with sBS. The effectiveness of Het-Nets' was also evaluated by considering on-grid mBSs whereas off-grid sBSs. Due to limited availability of transmit power, authors' findings suggest that off-grid sBSs give less coverage.

In [15], the authors have analyzed the performance of NOMA-based NU-HetNets. The authors have assessed the Dl coverage with energy efficiency. The results suggest that using NOMA in HetNets improves the energy efficiency as well as the coverage rate of the system.

Likewise, in [43] the authors consider the employment of RFA scheme in NU-Hetnets. The authors proposed muted sBSs in the proximity of mBSs for minimization of the co-tier interference. Moreover, for enhancing the edge coverage the sBSs are maintained functional in the mBS edge area.

2.9 Internet of Things

The Internet of Things (IoT) comprises a network of interconnected computing devices capable of transmitting data autonomously without the need for human-computer interaction. Smart homes, elder care, medical care, transportation, agri-

culture, and other areas can all benefit from IoT technology. [44] investigates the growing practice of integrating IoT with 5G networks. Furthermore, the authors assess the security implications of IoT-5G connectivity. The authors also explore the development IoT with 5G assistance in [45]. They also assess important enabling technologies and issues related to 5G supported IoT.

2.10 Thesis proposal

The following are some of the ways in which our approach varies from the current state of the art approaches:

1. In [18, 46], the authors have explored various jamming attacks across different network scenarios. Nevertheless, their research lacked an examination of deliberate jamming in HetNets. Hence, this study delves into the subject of deliberate jamming specifically within HetNets.

2. In [15, 16, 21, 22, 28], the authors use RFA in HetNets to mitigate the effect of ICI. However, the author have not assessed their system model under DJs-I. Therefore, in here, RFA is considered to minimize the effect of ICI as well as DJs-I.

3. In [15, 20, 28], DL coverage has been investigated. Here, our focus centers on analyzing the factors that influence the uplink (UL) coverage of Mobile End-Users (M-EUs).

4. In [47], the authors have studied interference mitigation in Hetnets using RFA. However, their proposed technique only deals with ICI. In this work, we investigate RFA for load balancing as well as mitigation of ICI and DJs-I.

CHAPTER 3

System Model

We consider a two tier HetNet where sBSs are deployed in the broadcasting region of mBS as shown in Fig. 1.1. Furthermore, this work introduces interference mitigation within the network layout schemes through Radio Frequency Allocation (RFA), in conjunction with a deliberate jamming mechanism employing intentional jammers. Certain mathematical foundations employed in this section will also find application in section 4 for deriving coverage probabilities.

3.1 Network Layout and Assumptions

A two-tier HetNets model has been suggested, featuring users, DJs, sBSs (small Base Stations), and mBSs (macro Base Stations). These entities, including users, DJs, sBSs, and mBSs, are represented through IHPPPs with their respective densities φ_{u}, φ_{J}, φ_S, and φ_{M}. Within the authorized communication spectrum, DJs emit unwanted energy, which detrimentally impacts network performance. It is assumed that the parameters of the network are known to the attackers so the UL communication can be targeted. DJs send undesirable energies in the legitimate transmission band, causing network performance to suffer. Single cluster of DJs is assumed to be around the target area which can have a significant jamming effect on the network. Moreover, only intra-cluster DJs-I has been examined which can simplify the analysis.

15

To mitigate DJs-I and ICI, a dynamic interference reduction technique known as Radio Frequency Allocation (RFA) is employed. In this context, a typical user is assumed. β represent the path loss constant and $|h|$ for the Rayleigh fading gain. User interaction is facilitated through the utilization of the maximum power scheme technique [48]. The effect of noise in the network has been neglected and only the effect of interference has been considered.

3.2 Deliberate Jamming Apparatus

DJs introduce interference in the permissible transmission band resulting in a reduced network coverage [18]. The DJs are randomly distributed within the broadcasting area of an mBS using IHPPP. Edge users situated far from the mBS encounter significant degradation in network performance due to Inter-Cell Interference (ICI) acting as a disruptive factor. Consequently, DJs disrupt the intended communication channel. Thus, with an increase in the number of DJs as well as the signal power, one can entirely jam the whole UL coverage of M-EUs.

Due to its wide-band nature, the noise power is likely to be less and cause little harm in the presence of a few DJs. As the density and power of the DJs rises, significant DJs-I is obtained, degrading the network's performance. [7, 49]. UL interactions of M-EUs in HetNets totally inhibited by increasing the density of DJs and transmission capacity.

3.3 Use of Reverse Frequency Allocation

The Soft Frequency Reuse (SFR) approach involves dividing the frequency band into two sub-bands. The first sub-band is allocated to users and sBSs positioned at the central area of the mBS's broadcasting range, while the second sub-band is designated for sBSs and users situated in the outer coverage zone of the mBS [16].RFA represents an advanced iteration of SFR with improved broadcast cov-

Bands \ Regions	Center Region A_l^g	Outer Region A_l^g
MBS F	$F_{1,DL}$ F_1 $F_{1,UL}$	$F_{2,DL}$ F_2 $F_{2,UL}$
SBS F'	$F'_{2,DL}$ F_2 $F'_{2,UL}$	$F'_{1,DL}$ F_1 $F'_{1,UL}$
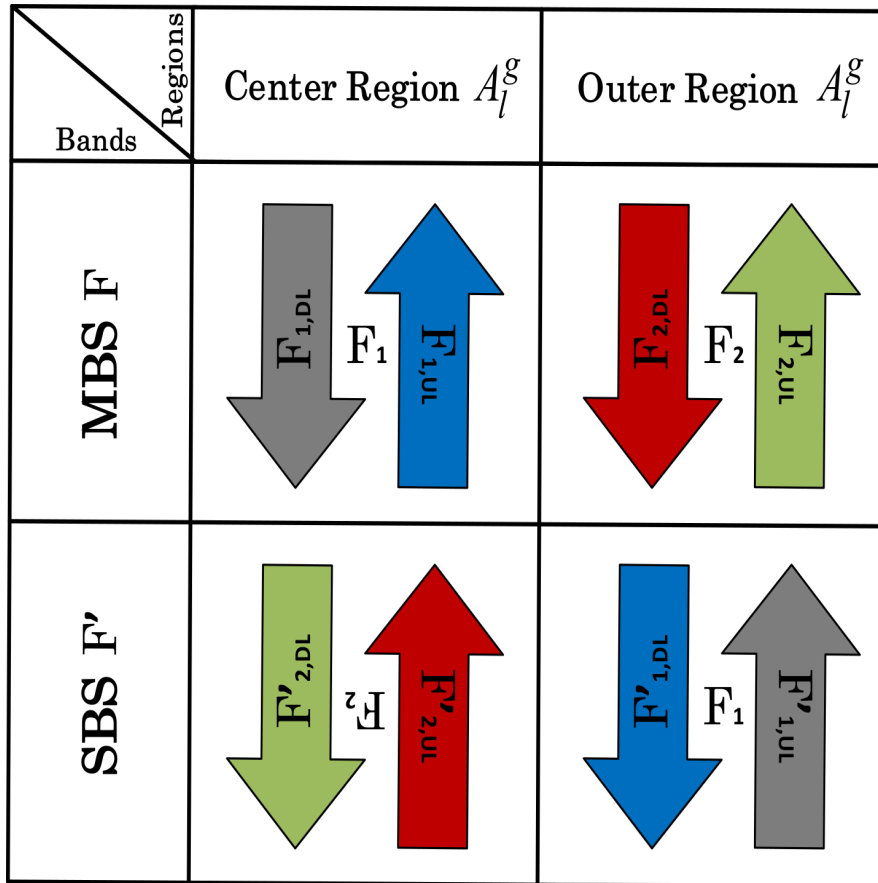
Figure 3.1: The depiction of a two-tier HetNet, coupled with Radio Frequency Allocation (RFA).

erage [50]. Within the framework of RFA, the frequency sub-bands are further subdivided into Uplink (UL) and Downlink (DL) bands, a feature not present in SFR. This division allows for significant interference reduction, surpassing the capabilities of SFR [28, 50]. The radio relay orientation of sBS is assigned in the opposite direction when compared to that of the mBS as shown in Fig. 3.1. The downlink (DL) frequencies of the mBS are allocated to the uplink (UL) of sBSs, while the uplink (UL) frequencies of the mBS are designated for the downlink (DL) of the sBSs [51]. Utilizing the RFA method substantially enhances the network capacity within the mBS coverage area. This form of frequency allocation effectively diminishes interference and greatly enhances spectral efficiency and network coverage. The allocation of frequency resources is optimized, resulting in reduced interference both within the same tier and across different tiers, while also signif-

icantly increasing the transmission rates [52].

In the context of RFA, there is no preassigned spectrum exclusively designated for sBSs. This approach mitigates interference and expands the coverage area. With the implementation of RFA, the entire spectrum of the mBS becomes available to sBSs, allocated in non-overlapping regions but in the opposite direction.

As shown in Fig. 3.1, for RFA, the sub-bands are employed in the opposite sequence for mBSs and sBSs, i.e., $A_l^g \ \forall \ l \in (\text{M}, \text{S})$ and $g \in (c, o)$[19].

To implement RFA, the allocated frequency band, denoted as F, is subdivided into two sub-bands, F_1 and F_2 such that $F = \bigcup_{z \in (1,2)} Fz$, as shown in Fig. 3.1. F_1 and F_2 these sub-bands are divided into uplink (UL) and downlink (DL) sub-carriers. These sub-bands are classified as: $F_1 = F_{1,\text{UL}} + F_{1,\text{DL}}$ and $F_2 = F_{2,\text{UL}} + F_{2,\text{DL}}$.

Proposed Technique

As ν is either located in A_{M}^c or in A_{M}^o, herein, we extricate the coverage probabilities for the following network scenarios.

1. Without RFA, the UL coverage probability when jammers are available, and

2. With RFA, the UL coverage probability when jammers are not present.

4.1 Without RFA the UL coverage probability when DJs are present

To disrupt the uplink communication of Mobile End-Users (M-EU) in HetNets, DJ-s are strategically placed in identical patterns around the broadcasting region of the mBS, employing IHPPP.The primary factors constraining efficiency in these networks are DJS-I and ICI. Hence, the equation for uplink coverage probability, $P_{A_{\mathrm{M}}^c}^{\mathrm{UL}}(\kappa_{\mathrm{M}})$, for mBS associating ν in A_{M}^c without the utilization of RFA and in the presence of DJ-s, the scenario can be described as follows:

$$P_{A_{\mathrm{M}}^c}^{\mathrm{UL}}(\kappa_{\mathrm{M}}) = P\left(\mathrm{SIR}_{\mathrm{M}}^{\mathrm{UL}} > \kappa_{\mathrm{M}}\right). \tag{4.1.1}$$

Here, κ_{M} is UL SIR threshold.Moreover $\mathrm{SIR}_{\mathrm{M}}^{\mathrm{UL}}$ represents the received UL SIR. $\mathrm{SIR}_{\mathrm{M}}^{\mathrm{UL}}$ from equation (4.1.1) it can be found as

$$\mathrm{SIR}_{\mathrm{M}}^{\mathrm{UL}} = \frac{P_{t,\nu}^{\mathrm{UL}}|h_{\mathrm{M}}|^2 r_{\mathrm{M}}^{-\beta}}{I_{\mathrm{M},A} + I_{\mathrm{S},A} + I_{J,A}},$$

$$= \frac{P_{t,\nu}^{\mathrm{UL}}|h_{\mathrm{M}}|^2 r_{\mathrm{M}}^{-\beta}}{\sum\limits_{l \in \phi_{\mathrm{M}}} P_{t,l}|h_l|^2 r_l^{-\beta} + \sum\limits_{k \in \phi_{\mathrm{S}}} P_{t,k}|h_k|^2 r_k^{-\beta} + \sum\limits_{j \in \phi_J} P_{t,j}|h_j|^2 r_j^{-\beta}}. \qquad (4.1.2)$$

In Eq(4.1.2), the UL interference in $A_{\mathrm{M}}^{\mathrm{c}}$ is the total number of mBS-tier interferences. $I_{\mathrm{M},A}$, sBS-tier $I_{\mathrm{S},A}$, and of DJs, $I_{J,A}$. $r_{(\cdot)}^{-\beta}$ represents the separation from either BS or DJs. However, $P_{t,\nu}^{\mathrm{UL}}$ represents the power transmitted in UL, whereas, $P_{t,k}, P_{t,l}$ and $P_{t,j}$ represents the powers transmitted of sBSs, mBSs, and DJs . φ_{S}, ϕ_{M} and φ_J represents the IHPPPs of sBSs, mBSs and DJs. Likewise, A denotes the broadcasting area of the mBS, $A = A_{\mathrm{M}}^{\mathrm{c}} \cup A_{\mathrm{M}}^{o}$. Using (4.1.2), (4.1.1) can be written as

$$P_{A_{\mathrm{M}}^{\mathrm{c}}}^{\mathrm{UL}}(\kappa_{\mathrm{M}}) = P\left(\frac{P_{t,\nu}^{\mathrm{UL}}|h_{\mathrm{M}}|^2 r_{\mathrm{M}}^{-\beta}}{I_{\mathrm{M},A} + I_{\mathrm{S},A} + I_{J,A}} > \kappa_{\mathrm{M}}\right)$$

$$= \mathrm{E}_{r_{\mathrm{M}}, I_{\mathrm{M},A}, I_{\mathrm{S},A}, I_{J,A}}\left[\exp\left(-\frac{r_{\mathrm{M}}^{\beta}\kappa_{\mathrm{M}}}{P_{t,\nu}^{\mathrm{UL}}}(I_{\mathrm{M},A} + I_{\mathrm{S},A} + I_{J,A})\right)\right]$$

$$= \mathrm{E}_{r_{\mathrm{M}}}\left[\mathcal{L}_{I_{\mathrm{M},A}}(s) \times \mathcal{L}_{I_{\mathrm{S},A}}(s) \times \mathcal{L}_{I_{J,A}}(s)\right]\Bigg|_{s=\frac{r_{\mathrm{M}}^{\beta}\kappa_{\mathrm{M}}}{P_{t,\nu}^{\mathrm{UL}}}}. \qquad (4.1.3)$$

Here, $\mathcal{L}_{I_{\mathrm{M},A}}(s), \mathcal{L}_{I_{\mathrm{S},A}}(s)$, and $\mathcal{L}_{I_{J,A}}(s)$ represent the LT of $I_{\mathrm{M},A}$, $I_{\mathrm{S},A}$, and $I_{J,A}$, respectively, whereas, the expectation of LT is given as $\mathrm{E}[\cdot]$.

In A, the LT of mBS-tier interference , $\mathcal{L}_{I_{\mathrm{M},A}}(s)$, is defined as

$$\mathcal{L}_{I_{\mathrm{M},A}}(s) =$$

$$\exp\left(\frac{\varphi_{\mathrm{M}}\pi\gamma_{\circ}\kappa_{\mathrm{M}}d_2^{(2-\beta)}r_{\mathrm{M}}^{\beta}}{\beta/2-1}{}_2F_1\left(1, 1-\frac{2}{\beta}, 2-\frac{2}{\beta}, -\gamma_{\circ}\kappa_{\mathrm{M}}\left(\frac{r_{\mathrm{M}}}{d_2}\right)^{\beta}\right) - \right.$$

$$\left.\frac{\varphi_{\mathrm{M}}\pi\gamma_{\circ}\kappa_{\mathrm{M}}y^{(2-\beta)}r_{\mathrm{M}}^{\beta}}{\beta/2-1}{}_2F_1\left(1, 1-\frac{2}{\beta}, 2-\frac{2}{\beta}, -\gamma_{\circ}\kappa_{\mathrm{M}}\left(\frac{r_{\mathrm{M}}}{y}\right)^{\beta}\right)\right). \qquad (4.1.4)$$

Proof: Proof of Eq. 4.1.4 is provided in Appendix A.1. Moreover, $\gamma_\circ = P_{t,\mathrm{M}}/P_{t,\nu}^{\mathrm{UL}}$, where $P_{t,\mathrm{M}}$ is transmission power of mBS-tier.

Similar to the approach used in (4.1.4), the $\mathcal{L}_{I_{\mathrm{S},A}}(s)$, is calculated as

$$\mathcal{L}_{I_{\mathrm{S},A}}(s) =$$

$$\exp\left(\frac{\varphi_{\mathrm{S}}\pi\gamma_1\kappa_{\mathrm{M}}x_2^{(2-\beta)}r_{\mathrm{M}}^\beta}{\beta/2-1}{}_2F_1\left(1,1-\frac{2}{\beta},2-\frac{2}{\beta},-\gamma_1\kappa\mathrm{M}\left(\frac{r_{\mathrm{M}}}{x_2}\right)^\beta\right) - \right.$$

$$\left.\frac{\varphi_{\mathrm{S}}\pi\gamma_1\kappa_{\mathrm{M}}x_1^{(2-\beta)}r_{\mathrm{M}}^\beta}{\beta/2-1}{}_2F_1\left(1,1-\frac{2}{\beta},2-\frac{2}{\beta},-\gamma_1\kappa_{\mathrm{M}}\left(\frac{r_{\mathrm{M}}}{x_1}\right)^\beta\right)\right). \tag{4.1.5}$$

Here, γ_1 is ratio of $P_{t,\mathrm{S}}$ and $P_{t,\nu}^{\mathrm{UL}}$, where $P_{t,\mathrm{S}}$ is the transmit power of SBS.

Similar to approached used in (4.1.4), the LT of the interference received from DJs, $\mathcal{L}_{I_J,A}(s)$, in A, can be given as

$$\mathcal{L}_{I_J,A}(s) =$$

$$\exp\left(\frac{\varphi_J\pi\gamma_2\kappa_{\mathrm{M}}z_2^{(2-\beta)}r_{\mathrm{M}}^\beta}{\beta/2-1}{}_2F_1\left(1,1-\frac{2}{\beta},2-\frac{2}{\beta},-\gamma_2\kappa_{\mathrm{M}}\left(\frac{r_{\mathrm{M}}}{z_2}\right)^\beta\right) - \right.$$

$$\left.\frac{\varphi_J\pi\gamma_2\kappa_{\mathrm{M}}z_1^{(2-\beta)}r_{\mathrm{M}}^\beta}{\beta/2-1}{}_2F_1\left(1,1-\frac{2}{\beta},2-\frac{2}{\beta},-\gamma_2\kappa_{\mathrm{M}}\left(\frac{r_{\mathrm{M}}}{z_1}\right)^\beta\right)\right). \tag{4.1.6}$$

Here, γ_2 is the ratio of $P_{t,J}$ and $P_{t,\nu}^{\mathrm{UL}}$ where the transmit power of DJs is $P_{t,J}$ and z_1 and z_2 are the jammers effective attacking regions, s.t., $z_1 \leq z_2$.

ν is located in A_{M}^c or in A_{M}^o (denoted as $\nu_{A_{\mathrm{M}}^c}$ and $\nu_{A_{\mathrm{M}}^o}$, respectively), while associated with mBS at a distance $r_{\mathrm{M},\nu}$, has PDFs of distances given, respectively, as (4.1.7) and (4.1.8) [53] [50]

$$f_{r_{\mathrm{M}}|\nu_{A_{\mathrm{M}}^c}}(r_{\mathrm{M}}) = \frac{2\pi\varphi_{\mathrm{M}}r_{\mathrm{M}}\exp(-\varphi_{\mathrm{M}}\pi r_{\mathrm{M}}^2)}{1-\exp\left(-\varphi_{\mathrm{M}}\pi d_1^2\right)}, \tag{4.1.7}$$

and

$$f_{r_{\mathrm{M}}|\nu_{A_{\mathrm{M}}^o}}(r_{\mathrm{M}}) = \frac{2\pi\varphi_{\mathrm{M}}r_{\mathrm{M}}\exp(-\varphi_{\mathrm{M}}\pi r_{\mathrm{M}}^2)}{\exp\left(-\varphi_{\mathrm{M}}\pi d_1^2\right)}. \tag{4.1.8}$$

UL coverage probability expression, $P_{A_\mathrm{M}^c}^{\mathrm{UL}}(\kappa_\mathrm{M})$, having uniformly deployed DJs without RFA for MBS associated ν in A_M^c, may be achieved as

$$P_{A_\mathrm{M}^c}^{\mathrm{UL}}(\kappa_\mathrm{M}) = \int_y^{d_1} \mathcal{L}_{I_{\mathrm{M},A}}(s) \times \mathcal{L}_{I_{\mathrm{S},A}}(s) \times \mathcal{L}_{I_{J,A}}(s)\, f_{r_{\mathrm{M},\nu}|\nu_{A_\mathrm{M}^c}}(r_{\mathrm{M},\nu})\, dr_{\mathrm{M},\nu}. \quad (4.1.9)$$

By substituting (4.1.4), (4.1.5), (4.1.6) and (4.1.7) into (4.1.9), $P_{A_\mathrm{M}^c}^{\mathrm{UL}}(\kappa_\mathrm{M})$ is achieved as (4.1.11).

Similarly, for mBS connected with ν in A_M^o, the UL coverage probability expression for uniformly distributed DJs without RFA, $P_{A_\mathrm{M}^o}^{\mathrm{UL}}(\kappa_\mathrm{M})$, is given as

$$P_{A_\mathrm{M}^o}^{\mathrm{UL}}(\kappa\mathrm{M}) = \int_{d_1}^{d_2} \mathcal{L}_{I_{\mathrm{M},A}}(s) \times \mathcal{L}_{I_{\mathrm{S},A}}(s) \times \mathcal{L}_{I_{J,A}}(s)\, f_{r_{\mathrm{M},\nu}|\nu_{A_\mathrm{M}^o}}(r_{\mathrm{M},\nu})\, dr_{\mathrm{M},\nu}. \quad (4.1.10)$$

By putting (4.1.4), (4.1.5), (4.1.6) and (4.1.8) in (4.1.10), $P_{A_\mathrm{M}^o}^{\mathrm{UL}}(\kappa_\mathrm{M})$ is written as (4.1.12).

4.2 With RFA the UL coverage probability when the DJS are present

The UL coverage probability, $P_{A_\mathrm{M}^c}^{\mathrm{UL},*}(\kappa_\mathrm{M})$, with DJs and RFA while considering ν in A_M^c can be written below

$$P_{A_\mathrm{M}^c}^{\mathrm{UL},*}(\kappa_\mathrm{M}) = P\left(\mathrm{SIR}_\mathrm{M}^{\mathrm{UL}} > \kappa_\mathrm{M}\right). \quad (4.2.1)$$

The total amount of UL interference experienced when using RFA is the sum of MBS-tier UL interference in A_M^c, i.e., $I_{\phi_\mathrm{M},A_\mathrm{M}^c}^{\mathrm{UL}}$, SBS-tier DL interference in A_M^o, i.e., $I_{\phi_i,A_\mathrm{M}^o}^{\mathrm{DL}}$, and interference from DJs, i.e., $I_{J,A}$. Therefore, $\mathrm{SIR}_\mathrm{M}^{\mathrm{UL}}$ from (4.2.1) can be written as

$$\mathrm{SIR}_\mathrm{M}^{\mathrm{UL}} = \frac{P_{t,\nu}^{\mathrm{UL}}|h_\mathrm{M}|^2 r_\mathrm{M}^{-\beta}}{I_{\phi_\mathrm{M},A_\mathrm{M}^c}^{\mathrm{UL}} + I_{\phi_\mathrm{S},A_\mathrm{M}^o}^{\mathrm{DL}} + I_{J,A}}. \quad (4.2.2)$$

$$P_{A_M^c}^{\text{UL}}(\kappa_M) = \frac{2\pi\varphi_M}{1-\exp\left(-\varphi_M\pi d_1^2\right)}\bigg|_y^{d_1} \exp\left(\frac{\pi\kappa_M r_M^\beta}{\beta/2-1}\left[\varphi_M\gamma_\circ d_2^{(2-\beta)}\mathcal{J}\left(\beta,-\kappa_M\gamma_\circ\left(\frac{r_M}{d_2}\right)^\beta\right)-\varphi_M\gamma_\circ y^{(2-\beta)}\mathcal{J}\left(\beta,-\kappa_M\gamma_\circ\left(\frac{r_M}{y}\right)^\beta\right)+\right.\right.$$

$$\varphi_S\gamma_1 x_2^{(2-\beta)}\mathcal{J}\left(\beta,-\kappa_M\gamma_1\left(\frac{r_M}{x_2}\right)^\beta\right)-\varphi_S\gamma_1 x_1^{(2-\beta)}\mathcal{J}\left(\beta,-\kappa_M\gamma_1\left(\frac{r_M}{x_1}\right)^\beta\right)+\varphi_J\gamma_2 z_2^{(2-\beta)}\mathcal{J}\left(\beta,-\kappa_M\gamma_2\left(\frac{r_M}{z_2}\right)^\beta\right)-$$

$$\left.\left.\varphi_J\gamma_2 z_1^{(2-\beta)}\mathcal{J}\left(\beta,-\kappa_M\gamma_2\left(\frac{r_M}{z_1}\right)^\beta\right)\right]-\varphi_M\pi r_M^2\right)r_M dr_M. \tag{4.1.11}$$

$$P_{A_M^o}^{\text{UL}}(\kappa_M) = \frac{2\pi\varphi_M}{\exp\left(-\varphi_M\pi d_1^2\right)^{d_1}}\bigg|^{d_2} \exp\left(\frac{\pi\kappa_M r_M^\beta}{\beta/2-1}\left[\varphi_M\gamma_\circ d_2^{(2-\beta)}\mathcal{J}\left(\beta,-\kappa_M\gamma_\circ\left(\frac{r_M}{d_2}\right)^\beta\right)-\varphi_M\gamma_\circ y^{(2-\beta)}\mathcal{J}\left(\beta,-\kappa_M\gamma_\circ\left(\frac{r_M}{y}\right)^\beta\right)\right.\right.$$

$$+\varphi_S\gamma_1 x_2^{(2-\beta)}\mathcal{J}\left(\beta,-\kappa M\gamma_1\left(\frac{r_M}{x_2}\right)^\beta\right)-\varphi_S\gamma_1 x_1^{(2-\beta)}\mathcal{J}\left(\beta,-\kappa_M\gamma_1\left(\frac{r_M}{x_1}\right)^\beta\right)+\varphi_J\gamma_2 z_2^{(2-\beta)}\mathcal{J}\left(\beta,-\kappa_M\gamma_2\left(\frac{r_M}{z_2}\right)^\beta\right)-$$

$$\left.\left.\varphi_J\gamma_2 z_1^{(2-\beta)}\mathcal{J}\left(\beta,-\kappa_M\gamma_2\left(\frac{r_M}{z_1}\right)^\beta\right)\right]-\varphi_M\pi r_M^2\right)r_M dr_M. \tag{4.1.12}$$

Equation (4.2.2) can be expanded as

$$\text{SIR}_M^{\text{UL}} =$$

$$\frac{P_{t,\nu}^{\text{UL}}|h_M|^2 r_M^{-\beta}}{\sum\limits_{l\in\phi_M}P_{t,l}^{\text{UL}}|h_l|^2 r_l^{-\beta}+\sum\limits_{k\in\phi_S}P_{t,k}^{\text{DL}}|h_k|^2 r_k^{-\beta}+\sum\limits_{j\in\phi_J}P_{t,j}|h_j|^2 r_j^{-\beta}}. \tag{4.2.3}$$

Here, $P_{t,l}^{\text{UL}}$, is the MBS UL transmit power of ν , and $P_{t,k}^{\text{DL}}$, is the SBS DL transmit power and $P_{t,j}$ is DJs transmit power . Further more, by putting (4.2.2) in (4.2.1),

we get $P_{A_{\mathrm{M}}^c}^{\mathrm{UL},*}(\kappa_{\mathrm{M}})$ as

$$P_{A_{\mathrm{M}}^c}^{\mathrm{UL},*}(\kappa_{\mathrm{M}}) = P\left(\frac{P_{t,\nu}^{\mathrm{UL}}|h_{\mathrm{M}}|^2 r_{\mathrm{M}}^{-\beta}}{I_{\phi_{\mathrm{M}},A_{\mathrm{M}}^c}^{\mathrm{UL}} + I_{\phi_{\mathrm{S}},A_{\mathrm{M}}^o}^{\mathrm{DL}} + I_{J,A}} > \kappa_{\mathrm{M}}\right)$$

$$= \mathrm{E}_{r_{\mathrm{M}},I_{\phi_{\mathrm{M}},A_{\mathrm{M}}^c}^{\mathrm{UL}},I_{\phi_{\mathrm{S}},A_{\mathrm{M}}^o}^{\mathrm{DL}},I_{J,A}}\left[\exp\left(-\frac{r_{\mathrm{M}}^\beta \kappa_{\mathrm{M}}}{P_{t,\nu}^{\mathrm{UL}}}\left(I_{\phi_{\mathrm{M}},A_{\mathrm{M}}^c}^{\mathrm{UL}}+I_{\phi_{\mathrm{S}},A_{\mathrm{M}}^o}^{\mathrm{DL}}+I_{J,A}\right)\right)\right]$$

$$= \mathrm{E}_{r_{\mathrm{M}}}\left[\mathcal{L}_{I_{\phi_{\mathrm{M}},A_{\mathrm{M}}^c}^{\mathrm{UL}}}(s) \times \mathcal{L}_{I_{\phi_{\mathrm{S}},A_{\mathrm{M}}^o}^{\mathrm{DL}}}(s) \times \mathcal{L}_{I_{J,A}}(s)\right]\bigg|_{s=\frac{r_{\mathrm{M}}^\beta \kappa_{\mathrm{M}}}{P_{t,\nu}^{\mathrm{UL}}}}. \qquad (4.2.4)$$

The Laplace Transform of MBS uplink interference in A_{M}^c, i.e., $\mathcal{L}_{I_{\phi_{\mathrm{M}},A_{\mathrm{M}}^c}^{\mathrm{UL}}}$, can be written as

$$\mathcal{L}_{I_{\phi_{\mathrm{M}},A_{\mathrm{M}}^c}^{\mathrm{UL}}} =$$

$$\exp\left(\frac{\varphi_{\mathrm{M}}\pi\kappa_{\mathrm{M}}d_1^{(2-\beta)}r_{\mathrm{M}}^\beta}{\beta/2-1}{}_2F_1\left(1,1-\frac{2}{\beta},2-\frac{2}{\beta},-\kappa_{\mathrm{M}}\left(\frac{r_{\mathrm{M}}}{d_1}\right)^\beta\right)-\right.$$

$$\left.\frac{\varphi_{\mathrm{M}}\pi\kappa_{\mathrm{M}}y^{(2-\beta)}r_{\mathrm{M}}^\beta}{\beta/2-1}{}_2F_1\left(1,1-\frac{2}{\beta},2-\frac{2}{\beta},-\kappa_{\mathrm{M}}\left(\frac{r_{\mathrm{M}}}{y}\right)^\beta\right)\right). \qquad (4.2.5)$$

Proof: See Appendix A.2 for the proof of (4.2.5).

Moreover, LT of SBS DL interference in A_{M}^o, i.e., $\mathcal{L}_{I_{\phi_{\mathrm{S}},A_{\mathrm{M}}^o}^{\mathrm{DL}}}$, can be written in a way similar to (4.2.5), and is given as

$$\mathcal{L}_{I_{\phi_{\mathrm{S}},A_{\mathrm{M}}^o}^{\mathrm{DL}}} = \mathcal{L}_{I_{\phi_{\mathrm{S}},A_{\mathrm{M}}^c}^{\mathrm{DL}}} =$$

$$\exp\left(\frac{\varphi_{\mathrm{S}}'\pi\gamma_3\kappa_{\mathrm{M}}x_2^{(2-\beta)}r_{\mathrm{M}}^\beta}{\beta/2-1}{}_2F_1\left(1,1-\frac{2}{\beta},2-\frac{2}{\beta},-\gamma_3\kappa_{\mathrm{M}}\left(\frac{r_{\mathrm{M}}}{x_2}\right)^\beta\right)-\right.$$

$$\left.\frac{\varphi_{\mathrm{S}}'\pi\gamma_3\kappa_{\mathrm{M}}x_1^{(2-\beta)}r_{\mathrm{M}}^\beta}{\beta/2-1}{}_2F_1\left(1,1-\frac{2}{\beta},2-\frac{2}{\beta},-\gamma_3\kappa_{\mathrm{M}}\left(\frac{r_{\mathrm{M}}}{x_1}\right)^\beta\right)\right). \qquad (4.2.6)$$

Here, $\mathcal{L}_{I_{\phi_{\mathrm{S}},A_{\mathrm{M}}^o}^{\mathrm{DL}}} = \mathcal{L}_{I_{\phi_{\mathrm{S}},A_{\mathrm{M}}^c}^{\mathrm{DL}}}$ because φ_{S} in A_{M}^c is approximately equal to φ_{S} in A_{M}^o. γ_3 is the ratio of $P_{t,\mathrm{S}}^{\mathrm{DL}}$ and $P_{t,\nu}^{\mathrm{UL}}$ where $P_{t,\mathrm{S}}^{\mathrm{DL}}$ is the SBSs DL transmit power.

$$P_{A_{\mathrm{M}}^{c}}^{\mathrm{UL},*}\left(\kappa_{\mathrm{M}}\right)=\frac{2\pi\varphi_{\mathrm{M}}}{1-\exp\left(-\varphi_{\mathrm{M}}\pi d_{1}^{2}\right)}\Big|_{y}^{d_{1}}\exp\left(\frac{\pi\kappa_{\mathrm{M}}r_{\mathrm{M}}^{\beta}}{\beta/2-1}\left[\varphi_{\mathrm{M}}d_{1}^{(2-\beta)}\mathcal{J}\left(\beta,-\kappa_{\mathrm{M}}\left(\frac{r_{\mathrm{M}}}{d_{1}}\right)^{\beta}\right)-\varphi_{\mathrm{M}}y^{(2-\beta)}\mathcal{J}\left(\beta,-\kappa_{\mathrm{M}}\left(\frac{r_{\mathrm{M}}}{y}\right)^{\beta}\right)+\right.$$

$$\varphi_{\mathrm{S}}'\gamma_{3}d_{2}^{(2-\beta)}\mathcal{J}\left(\beta,-\kappa_{\mathrm{M}}\gamma_{3}\left(\frac{r_{\mathrm{M}}}{d_{2}}\right)^{\beta}\right)-\varphi_{\mathrm{S}}'\gamma_{3}d_{1}^{\,(2-\beta)}\mathcal{J}\left(\beta,-\kappa_{\mathrm{M}}\gamma_{3}\left(\frac{r_{\mathrm{M}}}{d_{1}}\right)^{\beta}\right)+\varphi_{J}\gamma_{2}d_{2}^{(2-\beta)}\mathcal{J}\left(\beta,-\kappa_{\mathrm{M}}\gamma_{2}\left(\frac{r_{\mathrm{M}}}{d_{2}}\right)^{\beta}\right)-$$

$$\varphi_{J}\gamma_{2}y^{(2-\beta)}\mathcal{J}\left(\beta,-\kappa_{\mathrm{M}}\gamma_{2}\left(\frac{r_{\mathrm{M}}}{y}\right)^{\beta}\right)\Big]-\varphi_{\mathrm{M}}\pi r_{\mathrm{M}}^{2}\right)r_{\mathrm{M}}dr_{\mathrm{M}}. \tag{4.2.8}$$

$$P_{A_{\mathrm{M}}^{o}}^{\mathrm{UL},*}\left(\kappa_{\mathrm{M}}\right)=\frac{2\pi\varphi_{\mathrm{M}}}{\exp\left(-\varphi_{\mathrm{M}}\pi d_{1}^{2}\right)}\Big|_{d_{1}}^{d_{2}}\exp\left(\frac{\pi\kappa_{\mathrm{M}}r_{\mathrm{M}}^{\beta}}{\beta/2-1}\left[\varphi_{\mathrm{M}}d_{2}^{(2-\beta)}\mathcal{J}\left(\beta,-\kappa_{\mathrm{M}}\left(\frac{r_{\mathrm{M}}}{d_{2}}\right)^{\beta}\right)-\varphi_{\mathrm{M}}d_{1}^{\,(2-\beta)}\mathcal{J}\left(\beta,-\kappa_{\mathrm{M}}\left(\frac{r_{\mathrm{M}}}{d_{1}}\right)^{\beta}\right)+\right.$$

$$\varphi_{\mathrm{S}}'\gamma_{3}d_{1}^{(2-\beta)}\mathcal{J}\left(\beta,-\kappa_{\mathrm{M}}\gamma_{3}\left(\frac{r_{\mathrm{M}}}{d_{1}}\right)^{\beta}\right)-\varphi_{\mathrm{S}}'\gamma_{3}y^{(2-\beta)}\mathcal{J}\left(\beta,-\kappa_{\mathrm{M}}\gamma_{3}\left(\frac{r_{\mathrm{M}}}{y}\right)^{\beta}\right)+\varphi_{J}\gamma_{2}d_{2}^{(2-\beta)}\mathcal{J}\left(\beta,-\kappa_{\mathrm{M}}\gamma_{2}\left(\frac{r_{\mathrm{M}}}{d_{2}}\right)^{\beta}\right)-$$

$$\varphi_{J}\gamma_{2}y^{(2-\beta)}\mathcal{J}\left(\beta,-\kappa_{\mathrm{M}}\gamma_{2}\left(\frac{r_{\mathrm{M}}}{y}\right)^{\beta}\right)\Big]-\varphi_{\mathrm{M}}\pi r_{\mathrm{M}}^{2}\right)r_{\mathrm{M}}dr_{\mathrm{M}}. \tag{4.2.9}$$

From (4.2.5), LT of MBS DL interference in A_{M}^{o}, i.e., $\mathcal{L}_{I_{\phi_{\mathrm{M}},A_{\mathrm{M}}^{o}}^{\mathrm{UL}}}$, is obtained as

$$\mathcal{L}_{I_{\phi_{\mathrm{M}},A_{\mathrm{M}}^{o}}^{\mathrm{UL}}}\left(s\right)=$$

$$=\exp\left(\frac{\varphi_{\mathrm{M}}\pi\kappa_{\mathrm{M}}d_{2}^{(2-\beta)}r_{\mathrm{M}}^{\beta}}{\beta/2-1}{}_{2}F_{1}\left(1,1-\frac{2}{\beta},2-\frac{2}{\beta},-\kappa_{\mathrm{M}}\left(\frac{r_{\mathrm{M}}}{d_{2}}\right)^{\beta}\right)-\right.$$

$$\left.\frac{\varphi_{\mathrm{M}}\pi\kappa_{\mathrm{M}}d_{1}^{(2-\beta)}r_{\mathrm{M}}^{\beta}}{\beta/2-1}{}_{2}F_{1}\left(1,1-\frac{2}{\beta},2-\frac{2}{\beta},-\kappa_{\mathrm{M}}\left(\frac{r_{\mathrm{M}}}{d_{1}}\right)^{\beta}\right)\right). \tag{4.2.7}$$

UL coverage probability expression, $P_{A_{\mathrm{M}}^{c}}^{\mathrm{UL},*}\left(\kappa_{\mathrm{M}}\right)$, having uniformly distributed DJs with RFA for MBS associated ν in A_{M}^{c} may be given as

$$P_{A_{\mathrm{M}}^{c}}^{\mathrm{UL},*}\left(\kappa_{\mathrm{M}}\right)=\int_{y}^{d_{1}}\mathcal{L}_{I_{\phi_{\mathrm{M}},A_{\mathrm{M}}^{c}}^{\mathrm{UL}}}\left(s\right)\times\mathcal{L}_{I_{\phi_{\mathrm{S}},A_{\mathrm{M}}^{o}}^{\mathrm{DL}}}\left(s\right)\times\mathcal{L}_{I_{J,A}}\left(s\right)f_{r_{\mathrm{M},\nu}|\nu_{A_{\mathrm{M}}^{c}}}\left(r_{\mathrm{M},\nu}\right)dr_{\mathrm{M},\nu}. \tag{4.2.10}$$

By putting (4.1.6), (4.1.7), (4.2.5) and (4.2.6), in (4.2.10), $P_{A_{\mathrm{M}}^{c}}^{\mathrm{UL},*}\left(\kappa_{\mathrm{M}}\right)$ is expressed as (4.2.8). UL coverage probability, $P_{A_{\mathrm{M}}^{o}}^{\mathrm{UL},*}\left(\kappa_{\mathrm{M}}\right)$, having uniformly distributed DJs

with RFA for MBS associated ν in A_{M}^o, may be given as

$$P_{A_{\mathrm{M}}^o}^{\mathrm{UL},*}\left(\kappa_{\mathrm{M}}\right) = \int_{d_1}^{d_2} \mathcal{L}_{I_{\phi_{\mathrm{M}},A_{\mathrm{M}}^o}^{\mathrm{UL}}}\left(s\right) \times \mathcal{L}_{I_{\phi_{\mathrm{S}},A_{\mathrm{M}}^c}^{\mathrm{DL}}}\left(s\right) \times \mathcal{L}_{I_{J,A}}\left(s\right) f_{r_{\mathrm{M},\nu}|\nu_{A_{\mathrm{M}}^o}}\left(r_{\mathrm{M},\nu}\right) dr_{\mathrm{M},\nu}.$$

$$(4.2.11)$$

By putting (4.1.6), (4.1.8), (4.2.6) and (4.2.7) in (4.2.11), $P_{A_{\mathrm{M}}^o}^{\mathrm{UL},*}\left(\kappa_{\mathrm{M}}\right)$ is expressed as (4.2.9).

CHAPTER 5

Results and Discussions

This chapter explains the results of probabilities of UL coverage for ν in the following conditions

(i) Uplink coverage probability versus radius (coverage area) with DJs and no RFA.

(ii) Uplink coverage probability versus radius (coverage area) in the presence of DJs with RFA.

MATLAB 2019b was used to obtain the results. mBS, sBS, user, and DJ are treated as

$A = (2000 \text{ m})^2 \pi$,

$A = A_{\text{M}}^c \text{U} A_{\text{M}}^o$

Distribution of DJs is in following area

$A = \pi (50 \text{ m})^2$,s.t.

Additionally, the mBS trnasmit power =30 dBm, sBS transmits at 20 dBm, ν=10 dBm and DJs=10 dBm. Different variables, such as $P_{t,\nu}^{\text{UL}}$, φ_J, φ_{M}, φ_{S}, κ_{M}, and $P_{t,J}$, are analyzed for location of ν in A_{M}^o against UL coverage.

5.1 Comparison of Probability of UL Coverage in A_{M}^{o} vs β_{M}

Figure 5.1 shows coverage probability versus path loss exponent β_M. It is evident from the figure that coverage probability decreases as the path loss exponent increases, and conversely, it increases as the path loss exponent decreases.
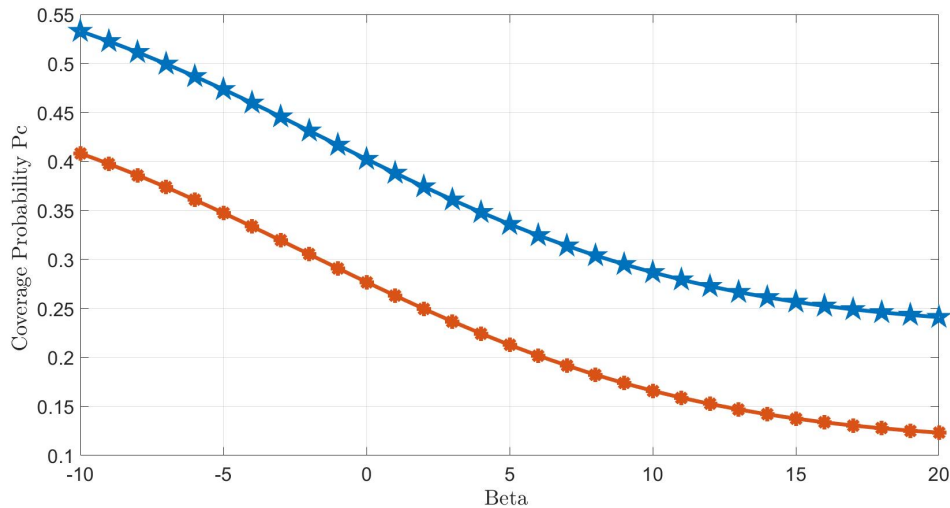

Figure 5.1: coverage probability vs pathloss exponent β

5.2 Comparison of Probability of UL Coverage in A_{M}^{o} vs κ_{M} and φ_{J} threshold

Figure 5.2 measures the probabilities of UL coverage in A_{M}^{o} versus different values of the κ_{M} and φ_{J} threshold. Generated for $\varphi_{J} = 0, 10, 20, 30, 40, 50$. Because of RFA's efficient use of resources and good interference mitigation, the figure illustrates that RFA enhances coverage. Due to large DJs-I φ_{J} produces considerable degradation of UL.

It can be seen in Fig. 5.2 that when $\varphi_{J} = 0$, the value of UL coverage starts from 0.62 and reduces to around 0.23. When the value of $\varphi_{J}=10$, the value of UL coverage starts from 0.6 and reduces to around 0.06. When the value of $\varphi_{J}=20$,

the value of UL coverage starts from 0.58 and reduces to around 0.02. When the value of φ_J=30, the value of UL coverage starts from 0.57 and reduces to around 0.01. When the value of φ_J=40, the value of UL coverage starts from 0.55 and reduces to around 0. When the value of φ_J=50, the value of UL coverage starts from 0.53 and reduces to around 0. It can be deduced from the figure that the quality of coverage reduces with increasing value of φ_J.
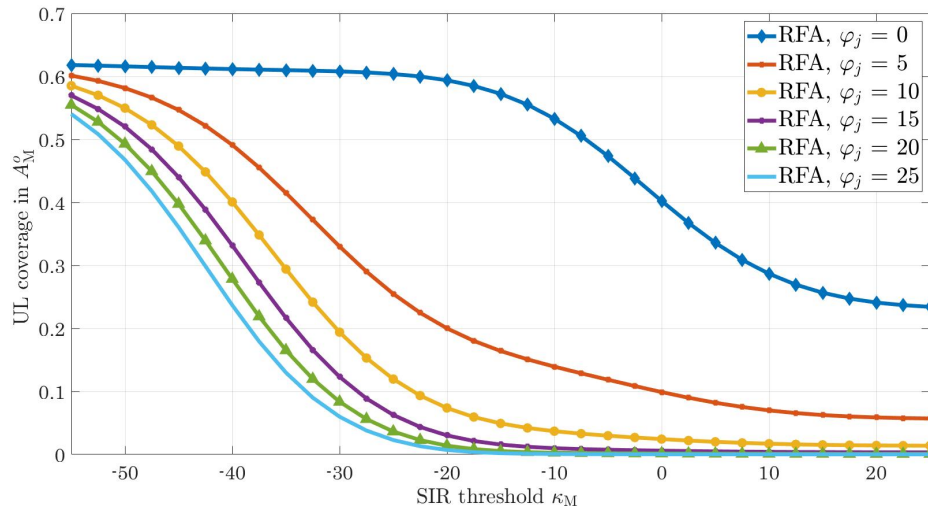

Figure 5.2: UL coverage against κ_{M} and φ_J in A_{M}^o.

5.3 For different DJs area radius against the Uplink coverage probabilities in $A_{\mathbf{M}}$

At Figs. 5.3 and 5.4, while assuming κ_{M} = -40 dB and φ_J = 10, 20, 30, 40 and 50, UL coverage probability in A_{M} is compared against DJs distribution area radius values. Graphs have been produced by examining various plausible scenarios, both with and without Radio Frequency Allocation (RFA). As a consequence of the findings, it can be inferred that expanding the distribution area of DJs improves UL coverage because of a reduction in the quantities of DJs per unit area, making DJs ineffective as long as their transmission power remains constant. However, RFA employment enhances UL coverage due to efficient resource allocation.
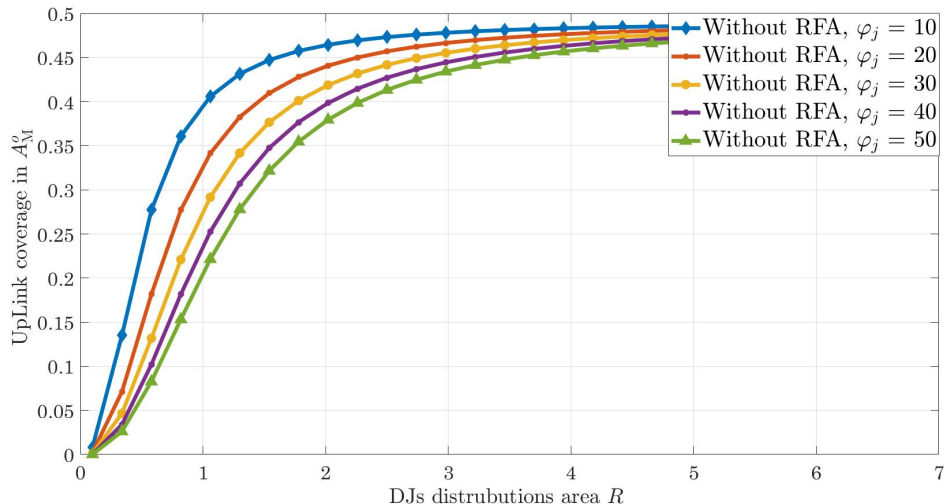
Fig. 5.3 shows a comparison between UL coverage and Djs distribution area
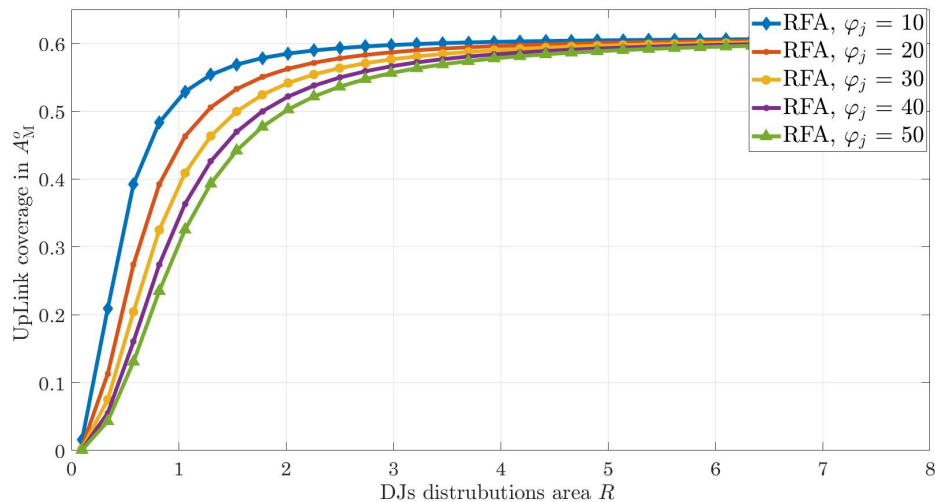
Figure 5.3: By employing RFA to encompass a DJ's distribution area, the uplink coverage against radius.

for different values of φ_J considering RFA. When the value of φ_J=10, the value of UL coverage increases from 0 to 0.6 with an increase in Djs distribution area up to 8. When the value of φ_J=20, the value of UL coverage increases from 0 to 0.59. When the value of φ_J=30, the value of UL coverage increases from 0 to 0.58. For φ_J=40, the UL coverage rises from 0 to 0.57, whereas, for φ_J=50, it increases from 0 to 0.56. It can be concluded that UL coverage improves as the DJs distribution area is increased.

Fig. 5.4 shows a comparison between UL coverage and Djs distribution area for different values of φ_J without RFA. When the value of φ_J=10, the value of UL coverage increases from 0 to 0.48 with an increase in Djs distribution area up to 6. For φ_J=20, the UL coverage probability goes from 0 to 0.47 whereas for φ_J=50, it goes from 0 to 0.44. As a result, it can be deduced that expanding the distribution area of DJs leads to improved UL coverage.

Figure 5.4: In absence of employing RFA to encompass a DJ's distribution area, the uplink coverage against radius.

5.4 Comparison of UL coverage probabilities in A_{M}^{o} vs different Djs area radius

Uplink coverage probabilities in A_{M}^{o} versus different Djs distribution area radius values are calculated in Figs. 5.5 and 5.6 while assuming $\varphi_{J} = 60$ and $\kappa_{\mathrm{M}} = $ -60, -40, -20, 0 and 20. Multiple scenarios with and without RFA have been considered while generating the plots. The increase in the area of Djs distribution reduces Djs-I because of wider distances. The results suggest that increasing the distribution area of the DJs improves UL coverage due to reduced DJs-I. However, the UL coverage probability reduces with an increase κ_{M} due to less user association.

Fig. 5.5 shows a comparison between UL coverage and Djs distribution area for different values of κ_{M} considering RFA. For $\kappa_{\mathrm{M}} = $ -60, the UL coverage goes from 0 to 0.62 by increasing the DJs distribution area to 8. Moreover, with $\kappa_{\mathrm{M}} = $ -40, the UL coverage rises from 0 to 0.59. With increasing κ_{M} to 0, UL coverage goes from 0 to 0.31, whereas, when κ_{M}=20, coverage is 0 to 0.19. It can be deduced that UL coverage is directly propositional to Djs distribution area.

Fig. 5.6 shows a comparison between UL coverage and DJs distribution area for different values of κ_{M} without RFA. When the value of κ_{M}=-60, the value of UL
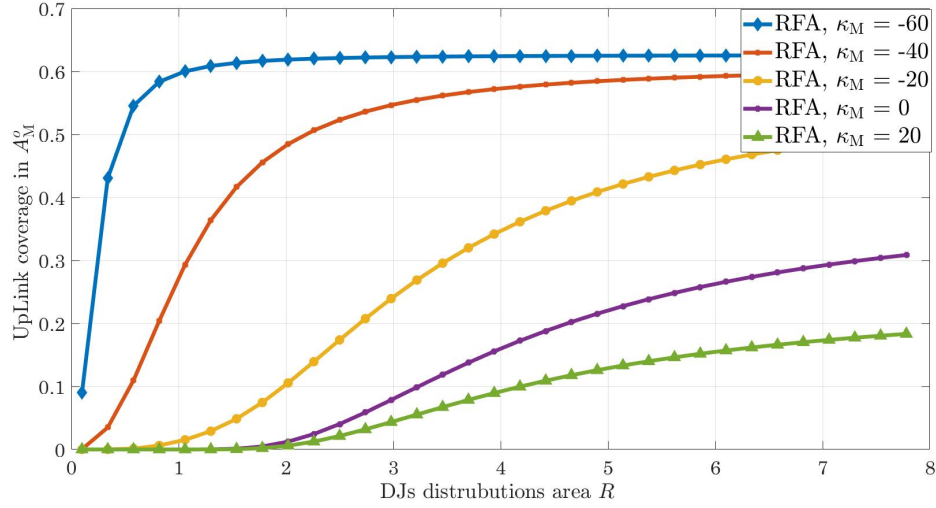
Figure 5.5: Within the DJ's distribution area, when RFA is deployed, the uplink (UL) coverage in relation to the radius.

coverage increases from 0 to 0.51 with an increase in the DJs distribution area up to 8. Moreover, with κ_M=-40, the UL coverage is 0 to 0.48. Likewise, for κ_M =-20 and κ_M=0, the UL coverage values are from 0 to 0.37 and 0 to 0.19, respectively. Similarly, for κ_M =20, UL coverage goes from 0 to 0.08. It can be concluded from the results that with an increase in the DJs distribution area, the UL coverage gets better.
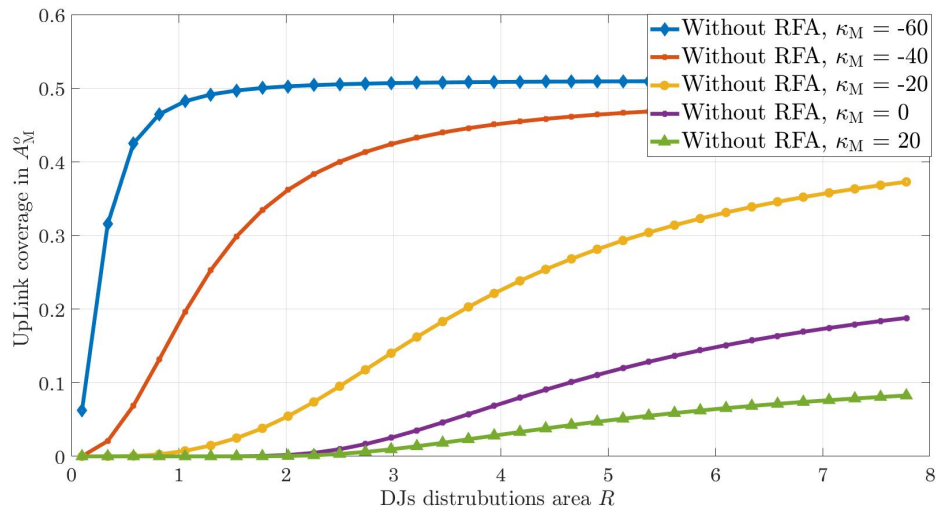

Figure 5.6: Within the DJs' distribution area, in the absence of RFA deployment, the uplink (UL) coverage in relation to the radius.

5.5 Discussion

Analysis of detailed results shows that the performance of the system has improved considerably with the addition of RFA. UL coverage is improved significantly by using RFA in the presence of Djs. Therefore, the proposed method of using RFA has considerably reduced the effect of DJs on UL communication.

5.6 Comparison with previous work

Figure 5.7 shows a comparison of the Probability of UL Coverage vs Distribution Area of Jammers with previous work [14]. C=3 and C=6 are the values taken from previous work. The figure shows that the UL coverage significantly improves as well as an increase in the distribution areas as compared to previous work.Therefore our work outperforms previous work.
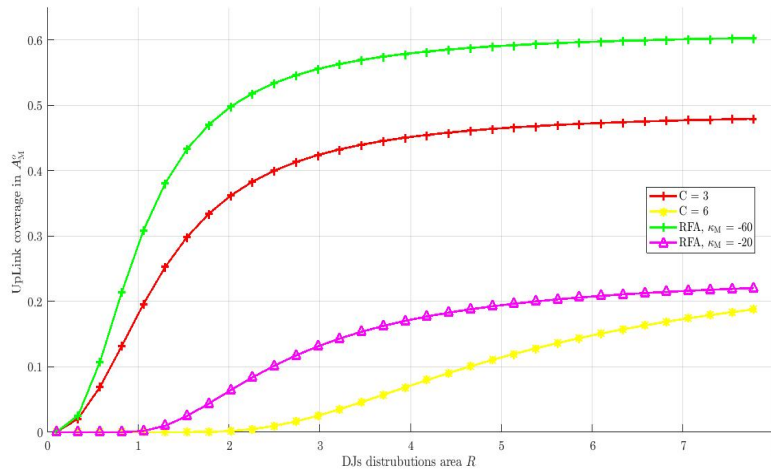
Figure 5.7: Comparison of Probability of UL Coverage vs Distribution Area of Jammers with previous Work.

CHAPTER 6

Conclusion

In HetNets, the UL coverage is limited by ICI. The situation gets worse when a deliberate jammer is present in the proximity of a target user. Herein, we proposed RFA to mitigate the effect of ICI and DJs-I. For a standardized Hetnet, IHPPPs was used to deploy mBS, sBSs, Users, and the DJs. Simulation results were obtained for different network parameters such as jammers transmit power, SINR threshold, distance, and transmit power of the mBS and sBSs for a system with RFA and without RFA, in the presence of DJs. It can be seen from the simulation results that the UL coverage deteriorates when the DJs are densely deployed in the proximity of the target as well as when their transmit power is high. Moreover, the results also show that in the presence of DJs, HetNet with RFA has improved UL coverage as compared to those without RFA.

A.1 Proof of the LT of (4.1.4)

Proof of (4.1.4):

from MBS-tier the LT of received interference $\mathcal{L}_{I_{M,A}}(s)$, in A, can be derived as

$$\mathcal{L}_{I_{M,A}}(s) = \mathrm{E}_{I_{M,A}}\left[\exp\left(-I_{M,A}s\right)\right]\Bigg|_{s=\frac{r_M^\beta \Gamma_M}{P_{t,\nu}^{UL}}}$$

$$= \mathrm{E}_{I_{M,A},|h_l|^2}\left[\exp\left(-s\sum_{l\in\phi_M} P_{t,M}|h_l|^2 r_l^{-\beta}\right)\right]$$

$$\stackrel{(a)}{\approx} \mathrm{E}_{I_{M,A},|h_l|^2}\left[\prod_{l\in\phi_M}\exp\left(-|h_l|^2\gamma_\circ\Gamma_M r_M^\beta r_l^{-\beta}\right)\right]$$

$$\stackrel{(b)}{\approx} \mathrm{E}_{I_{M,A}}\left[\prod_{l\in\phi_M}\mathrm{E}_{|h_l|^2}\exp\left(-|h_l|^2\gamma_\circ\Gamma_M r_M^\beta r_l^{-\beta}\right)\right]$$

$$\stackrel{(c)}{\approx} \mathrm{E}_{I_{M,A}}\left[\prod_{l\in\phi_M}\frac{1}{1+\gamma_\circ\Gamma_M\left(\frac{r_l}{r_M}\right)^{-\beta}}\right]$$

$$\stackrel{(d)}{\approx} \exp\left(-2\pi\rho_M y^{d2}\frac{r_l dr_l}{1+\left(\frac{r_l}{(\gamma_\circ\Gamma_M)^{1/\beta} r_M}\right)^\beta}\right)$$

$$\stackrel{(e)}{\approx} \exp\left(-\pi\rho_M(\gamma_\circ\Gamma_M)^{2/\beta} r_M^2 \frac{\left(\frac{d_2}{\gamma_\circ\Gamma_M^{1/\beta} r_M}\right)^2}{\left(\frac{y}{(\gamma_\circ\Gamma_M)^{1/\beta} r_M}\right)^2}\frac{du}{1+(u)^{\beta/2}}\right)$$

Here, Step (a) is obtained through the Laplace transform's definition., Step (c) is

acquired by LT of Step (b) with respect to h_j, Step (d) is acquired by applying probability generating functional (PGFL) of IHPPP [48], Step (e) is acquired by putting the value of $u = \left(\dfrac{r_l}{(\gamma_\circ \Gamma_{\mathrm{M}})^{1/\beta} \, r_{\mathrm{M}}} \right)^2$ in Step (d). Ultimately, (4.1.4) is obtained by computing the Gauss-hypergeometric approximation of Step (e).

A.2 Proof of the LT of (4.2.5)

Proof of (4.2.5):

$$\mathcal{L}_{I^{\mathrm{UL}}_{\phi_{\mathrm{M}}, A^c_{\mathrm{M}}}}(s) = \mathrm{E}_{I^{\mathrm{UL}}_{\phi_{\mathrm{M}}, A^c_{\mathrm{M}}}} \left[\exp\left(-I^{\mathrm{UL}}_{\phi_{\mathrm{M}}, A^c_{\mathrm{M}}} s \right) \right] \Bigg|_{s = \frac{r^{\beta}_{\mathrm{M}} \Gamma_{\mathrm{M}}}{P^{\mathrm{UL}}_{t,\nu}}}$$

$$= \mathrm{E}_{I^{\mathrm{UL}}_{\phi_{\mathrm{M}}, A^c_{\mathrm{M}}}, |h_l|^2} \left[\exp\left(-s \sum_{l \in \phi_{\mathrm{M}}} P^{\mathrm{UL}}_{t,\nu} |h_l|^2 r_l^{-\beta} \right) \right]$$

$$= \mathrm{E}_{I^{\mathrm{UL}}_{\phi_{\mathrm{M}}, A^c_{\mathrm{M}}}, |h_l|^2} \left[\prod_{l \in \phi_{\mathrm{M}}} \exp\left(-|h_l|^2 \Gamma_{\mathrm{M}} r^{\beta}_{\mathrm{M}} r_l^{-\beta} \right) \right]$$

$$= \mathrm{E}_{I^{\mathrm{UL}}_{\phi_{\mathrm{M}}, A^c_{\mathrm{M}}}} \left[\prod_{l \in \phi_{\mathrm{M}}} \mathrm{E}_{|h_l|^2} \exp\left(-|h_l|^2 \Gamma_{\mathrm{M}} r^{\beta}_{\mathrm{M}} r_l^{-\beta} \right) \right]$$

$$= \mathrm{E}_{I^{\mathrm{UL}}_{\phi_{\mathrm{M}}, A^c_{\mathrm{M}}}} \left[\prod_{l \in \phi_{\mathrm{M}}} \frac{1}{1 + \Gamma_{\mathrm{M}} \left(\dfrac{r_l}{r_{\mathrm{M}}} \right)^{-\beta}} \right]$$

$$= \exp\left(-2\pi \rho_{\mathrm{M}} \int_{y}^{d_1} \frac{r_l \, dr_l}{1 + \left(\dfrac{r_l}{\Gamma^{1/\beta}_{\mathrm{M}} r_{\mathrm{M}}} \right)^{\beta}} \right)$$

$$\overset{(f)}{\approx} \exp\left(-\pi \rho_{\mathrm{M}} \Gamma^{2/\beta}_{\mathrm{M}} r^2_{\mathrm{M}} \int_{\left(\frac{y}{\Gamma^{1/\beta}_{\mathrm{M}} r_{\mathrm{M}}} \right)^2}^{\left(\frac{d_1}{\Gamma^{1/\beta}_{\mathrm{M}} r_{\mathrm{M}}} \right)^2} \frac{du}{1 + (u)^{\beta/2}} \right)$$

Ultimately, through the computation of the Gaussian hypergeometric approximation of Step (f) we reach the following:t (4.2.5).

References

[1] H. G. Youngjun Xu, Guan Gui and F. Adachi, "A survey on resource allocation for 5g heterogeneous networks: current research, future trends, and challenges," *IEEE communications surveys and tutorials*, 2021.

[2] B. Soret, A. De Domenico, S. Bazzi, N. H. Mahmood, and K. I. Pedersen, "Interference coordination for 5G new radio," *IEEE Wireless Communications*, vol. 25, no. 3, pp. 131–137, 2017.

[3] S. Zou, N. Liu, Z. Pan, and X. You, "Joint power and resource allocation for non-uniform topologies in heterogeneous networks," in *proc. 83rd Vehicular Technology Conference (VTC Spring).* IEEE, 2016, pp. 1–5.

[4] J. Mirkovic and P. Reiher, "A taxonomy of ddos attack and ddos defense mechanisms," *ACM SIGCOMM Computer Communication Review*, vol. 34, no. 2, pp. 39–53, 2004.

[5] R. P. Jover, "Security attacks against the availability of LTE mobility networks: Overview and research directions," in *proc. International Symposium on Wireless Personal Multimedia Communication (WPMC).* IEEE, 2013, pp. 1–9.

[6] Y. Huo, X. Fan, L. Ma, X. Cheng, Z. Tian, and D. Chen, "Secure communications in tiered 5G wireless networks with cooperative jamming," *IEEE Trans. on Wireless Commun.*, 2019.

[7] W. Jundong, "Complex environment noise barrage jamming effects on air-

References

borne warning radar," *American J. of Remote Sensing*, vol. 6, no. 2, pp. 59–63, 2018.

[8] C. V. Ham and T. E. Scoughton, "Radio frequency jammer," Jan. 15 2008, US Patent 7,318,368.

[9] A. Viterbi, "A robust ratio-threshold technique to mitigate tone and partial band jamming in coded MFSK systems," in *proc. MILCOM 1982-IEEE Military Communications Conference-Progress in Spread Spectrum Communications*, vol. 1.   IEEE, 1982, pp. 22–4.

[10] S. Wang, Y. Gao, N. Sha, G. Zhang, and G. Zang, "Physical layer security in k-tier heterogeneous cellular networks over nakagami-m channel during uplink and downlink phases," *IEEE Access*, vol. 7, pp. 14 581–14 592, 2019.

[11] J. G. Andrews, S. Buzzi, W. Choi, S. V. Hanly, A. Lozano, A. C. Soong, and J. C. Zhang, "What will 5G be?" *IEEE Journal on Selected Areas in Communications*, vol. 32, no. 6, pp. 1065–1082, 2014.

[12] Z. H. Abbas, G. Abbas, M. S. Haroon, F. Muhammad, and S. Kim, "Proactive uplink interference mitigation in hetnets stressed by uniformly distributed wideband jammers," *Electronics*, vol. 8, no. 12, p. 1496, 2019.

[13] B. Błaszczyszyn, M. Haenggi, P. Keeler, and S. Mukherjee, *Stochastic geometry analysis of cellular networks*.   Cambridge University Press, 2018.

[14] F. Muhammad, M. S. Haroon, Z. H. Abbas, G. Abbas, and S. Kim, "Uplink interference management for hetnets stressed by clustered wide-band jammers," *IEEE Access*, vol. 7, pp. 182 679–182 690, 2019.

[15] T. Han, J. Gong, X. Liu, S. R. Islam, Q. Li, Z. Bai, and K. S. Kwak, "On downlink NOMA in heterogeneous networks with non-uniform small cell deployment," *IEEE Access*, vol. 6, pp. 31 099–31 109, 2018.

REFERENCES

[16] M. S. Haroon, Z. H. Abbas, G. Abbas, and F. Muhammad, "Coverage analysis of ultra-dense heterogeneous cellular networks with interference management," *Wireless Networks*, pp. 1–13, 2019.

[17] S. Hashima, O. Muta, M. Alghonimey, H. Shalaby, H. Frukawa, S. Elnoubi, and I. Mahmoud, "Area spectral efficiency performance comparison of downlink fractional frequency reuse schemes for MIMO heterogeneous networks," in *proc. International Conference on Information Science, Electronics and Electrical Engineering*, vol. 2. IEEE, 2014, pp. 1005–1010.

[18] M. Lichtman, J. D. Poston, S. Amuru, C. Shahriar, T. C. Clancy, R. M. Buehrer, and J. H. Reed, "A communications jamming taxonomy," *IEEE Security and Privacy*, vol. 14, no. 1, pp. 47–54, 2016.

[19] M. I. F. M. S. K. Muhammad Qasim, Muhammad Sajid Haroon, "5g cellular networks: Coverage analysis in the presence of inter-cell interference and intentional jammers," *Electronics*, vol. 9, no. 9, p. 1538, 2020.

[20] F. Y. L. Fazal Muhammad, Ziaul Haq Abbas, "Cell association with load balancing in nonuniform heterogeneous cellular networks: Coverage probability and rate analysis," *IEEE Transactions on Vehicular Technology*, vol. 66, pp. 5241–5255, 2016.

[21] F. M. L. J. Muhammad Mussawer Pervez, Ziaul Haq Abbas, "Location-based coverage and capacity analysis of a two tier HetNet," *IET Communications*, vol. 11, pp. 1067–1073, 2016.

[22] L. J. Ziaul Haq Abbas, Fazal Muhammad, "Analysis of load balancing and interference management in heterogeneous cellular networks," *IEEE Access*, vol. 5, pp. 14 690–14 705, 2017.

[23] J. J. J. S. Poongup Lee, Taeyoung Lee, "Interference management in lte femtocell systems using fractional frequency reuse," in *The 12th International Conference on Advanced Communication Technology (ICACT)Gangwon, Korea (South)*. IEEE, 2010, pp. 1047–1051.

39

REFERENCES

[24] T. T. Do, E. Björnson, E. G. Larsson, and S. M. Razavizadeh, "Jamming-resistant receivers for the massive mimo uplink," *IEEE Transactions on Information Forensics and Security*, vol. 13, no. 1, pp. 210–223, 2017.

[25] K. Grover, A. Lim, and Q. Yang, "Jamming and anti-jamming techniques in wireless networks: A survey," *Int. J. of Ad Hoc and Ubiquitous Comput.*, vol. 17, no. 4, pp. 197–215, 2014.

[26] S.-M. Tseng, Y.-F. Chen, P.-H. Chiu, and H.-C. Chi, "Jamming resilient cross-layer resource allocation in uplink harq-based simo ofdma video transmission systems," *IEEE Access*, vol. 5, pp. 24 908–24 919, 2017.

[27] F. M. Muhammad Sajid Haroon, G. Abbas, Z. H. Abbas, A. K. Hassan, M. Waqas, and S. Kim, "Interference management in ultra-dense 5g networks with excessive drone usage," *IEEE Access*, vol. 8, pp. 102 155–102 164, 2020.

[28] A. Ijaz, S. A. Hassan, S. A. R. Zaidi, D. N. K. Jayakody, and S. M. H. Zaidi, "Coverage and rate analysis for downlink HetNets using modified reverse frequency allocation scheme," *IEEE Access*, vol. 5, pp. 2489–2502, 2017.

[29] N. Hassan and X. Fernando, "Massive mimo wireless networks: An overview," *Electronics*, vol. 6, no. 3, p. 63, 2017.

[30] R. W. Heath, M. Kountouris, and T. Bai, "Modeling heterogeneous network interference using poisson point processes," *IEEE Transactions on Signal Processing*, vol. 61, no. 16, pp. 4114–4126, 2013.

[31] H. S. Dhillon, M. Kountouris, and J. G. Andrews, "Downlink mimo hetnets: Modeling, ordering results and performance analysis," *IEEE Transactions on Wireless Communications*, vol. 12, no. 10, pp. 5208–5222, 2013.

[32] W. Xu and H. Zhang, "Uplink interference mitigation for heterogeneous networks with user-specific resource allocation and power control," *EURASIP Journal on Wireless Communications and Networking*, vol. 2014, no. 1, p. 55, 2014.

REFERENCES

[33] M. Hefnawi, "Hybrid beamforming for millimeter-wave heterogeneous networks," *Electronics*, vol. 8, no. 2, p. 133, 2019.

[34] N. Naganuma, S. Nakazawa, S. Suyama, Y. Okumura, and H. Otsuka, "Performance evaluation of adaptive control cre in hetnet with eicic scheme," *IEICE Communications Express*, vol. 6, no. 4, pp. 166–171, 2017.

[35] A. G. Vikram Chandrasekhar, Jeffrey G. Andrews, "Femtocell networks: a survey," *IEEE Communications Magazine*, vol. 46, pp. 59–67, 2008.

[36] N. Deng, W. Zhou, and M. Haenggi, "Outage and capacity of heterogeneous cellular networks with intra-tier dependence," in *2014 Sixth International Conference on Wireless Communications and Signal Processing (WCSP)*. IEEE, 2014, pp. 1–5.

[37] A. Haider and S.-H. Hwang, "Maximum transmit power for ue in an lte small cell uplink," *Electronics*, vol. 8, no. 7, p. 796, 2019.

[38] H. Munir, S. A. Hassan, H. Pervaiz, Q. Ni, and L. Musavian, "User association in 5g heterogeneous networks exploiting multi-slope path loss model," in *2017 2nd Workshop on recent trends in telecommunications research (RTTR)*. IEEE, 2017, pp. 1–5.

[39] X. Zhang and J. G. Andrews, "Downlink cellular network analysis with multi-slope path loss models," *IEEE Transactions on Communications*, vol. 63, no. 5, pp. 1881–1894, 2015.

[40] L. Guo, S. Cong, and Z. Sun, "Multichannel analysis of soft frequency reuse and user association in two-tier heterogeneous cellular networks," *EURASIP Journal on Wireless Communications and Networking*, vol. 2017, no. 1, pp. 1–20, 2017.

[41] M. Fereydooni, M. Sabaei, M. Dehghan, G. B. Eslamlou, and M. Rupp, "Analytical evaluation of heterogeneous cellular networks under flexible user association and frequency reuse," *Computer Communications*, vol. 116, pp. 147–158, 2018.

REFERENCES

[42] K.-H. Liu and T.-Y. Yu, "Performance of off-grid small cells with non-uniform deployment in two-tier HetNet," *IEEE Transactions on Wireless Communications*, vol. 17, no. 9, pp. 6135–6148, 2018.

[43] F. Muhammad, Z. H. Abbas, and F. Y. Li, "Cell association with load balancing in nonuniform heterogeneous cellular networks: Coverage probability and rate analysis," *IEEE Transactions on Vehicular Technology*, vol. 66, no. 6, pp. 5241–5255, 2016.

[44] W. Ejaz, A. Anpalagan, M. A. Imran, M. Jo, M. Naeem, S. B. Qaisar, and W. Wang, "Internet of Things (IoT) in 5G wireless communications," *IEEE Access*, vol. 4, pp. 10 310–10 314, 2016.

[45] S. Li, L. Da Xu, and S. Zhao, "5G Internet of Things: A survey," *Journal of Industrial Information Integration*, vol. 10, pp. 1–9, 2018.

[46] Q. Y. Kanika Grover, Alvin Lim, "Jamming and anti-jamming techniques in wireless networks: a survey," in *International Journal of Ad Hoc and Ubiquitous Computing*, vol. 17, 2013, pp. 197–2015.

[47] L. J. Fazal Muhammad, Ziaul Haq Abbas, "Analysis of interference avoidance with load balancing in heterogeneous cellular networks," *2016 IEEE 27th Annual International Symposium on Personal, Indoor, and Mobile Radio Communications (PIMRC)*, 2016.

[48] X. Jiang, B. Zheng, W.-P. Zhu, L. Wang, and Y. Zou, "Large system analysis of heterogeneous cellular networks with interference alignment," *IEEE Access*, vol. 6, pp. 8148–8160, 2018.

[49] S. Gecgel, C. Goztepe, and G. K. Kurt, "Jammer detection based on artificial neural networks: A measurement study," in *Proc. of the ACM Workshop on Wireless Security and Machine Learning*, 2019, pp. 43–48.

[50] M. S. Haroon, Z. H. Abbas, F. Muhammad, and G. Abbas, "Coverage analysis of cell-edge users in heterogeneous wireless networks using Stienen's

model and RFA scheme," *International Journal of Communication Systems*, p. e4147.

[51] A. J. Ponnu Jacob and A. Madhukumar, "Downlink capacity improvement and interference reduction through reverse frequency allocation," in *2012 IEEE International Conference on Communication Systems (ICCS)*, 2012, pp. 329–333.

[52] M. A. S. W. K. N. M. S. H. S. Qureshi, "Clustered jamming in aerial hetnets with decoupled access," *IEEE Access*, vol. 8, pp. 142 218–142 228, 2020.

[53] M. Haenggi, *Stochastic geometry for wireless networks.* Cambridge University Press, 2012.